Theoretical Study of the Addition of Hydrogen Cyanide to Methanimine in the Gas Phase and in Aqueous Solution

Roger Arnaud,[†] Carlo Adamo,[‡] Maurizio Cossi,[‡] Anne Milet,[†] Yannick Vallée,[†] and Vincenzo Barone*,[‡]

Contribution from the Laboratoire d'Etudes Dynamiques et Structurales de la Sélectivité (LEDSS), UMR CNRS 5616, Université Joseph Fourier, 301 Avenue de la Chimie, BP 53X, F-38041 Grenoble Cedex 09, France, and Dipartimento di Chimica, Università "Federico II", via Mezzocannone 4, I-80134 Napoli, Italy

Received April 8, 1999. Revised Manuscript Received November 2, 1999

Abstract: We have performed a detailed study of the title reaction, which is the key step of one of the most realistic processes suggested for the prebiotic synthesis of amino acids. From a methodological point of view, our results confirm the reliability of the integrated computational tool formed by the B3LYP density functional model and the polarizable continuum model for the description of solvent effects. From a more chemical point of view, the reaction is quite unlikely in the gas phase due to the presence of significant reaction barriers, whereas the aqueous medium leads to a more feasible mechanism thanks to the preferential solvation of zwitterionic transition structures. Both specific and bulk solvent effects play a role in determining the overall mechanism.

Introduction

In the Strecker synthesis, an α-amino acid is formed by treatment of an aldehyde by hydrogen cyanide in the presence of aqueous ammonia.[1] This reaction, which is of great practical interest,[2,3] has been proposed as the prebiotic process by which amino acids appeared on the primitive earth.[4] In his famous experiment,[5] Miller obtained various amino acids by sparking mixtures of CH_4, NH_3, H_2O, and H_2. He proposed that aldehydes and HCN were formed in the sparks and then dissolved in water, where they further reacted to give inter alia amino acids.[6] Because the precise composition of the prebiotic earth atmosphere is still a matter of debate, such experiments have been repeated using various gas mixtures and varying the energy sources.[4] However, and even though alternative routes to amino acids have been proposed,[7] the possibility of a prebiotic Strecker synthesis still remains as a realistic and seductive hypothesis.

Strecker precursors for the simplest α-amino acid, glycine, are formaldehyde, hydrogen cyanide, ammonia, and water. Scheme 1 summarizes the possible reactions with this four-component mixture.

Scheme 1

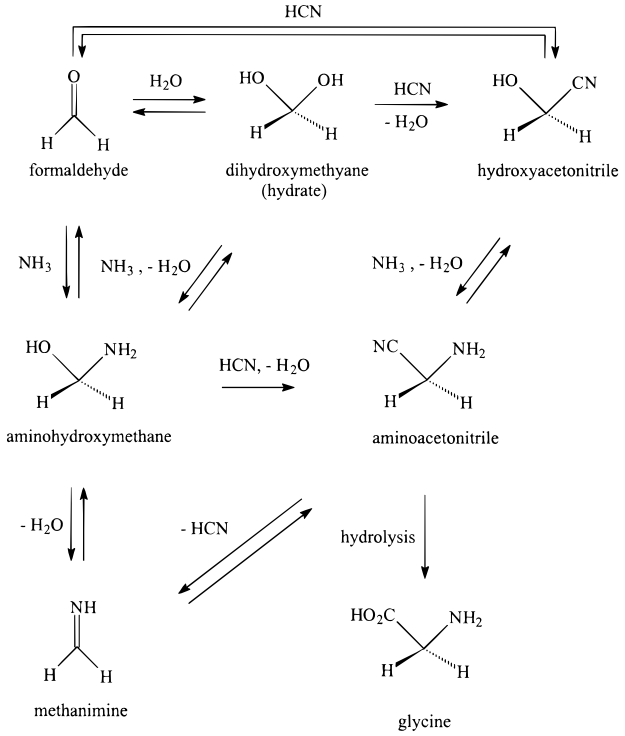

Aminoacetonitrile is the central crossroads of the system. Upon hydrolysis, it leads to the final amino acid, and it can be formed in three ways from formaldehyde: (i) by addition of HCN followed by nucleophilic substitution of the hydroxy group of hydroxyacetonitrile by ammonia; (ii) by addition of ammonia, forming aminohydroxymethane in which the OH group is then replaced by a CN; (iii) alternatively, aminohydroxymethane can be first dehydrated to methanimine, which then undergoes a nucleophilic addition of hydrogen cyanide. The hydrate, result-

* To whom correspondence should be addressed. E-mail: enzo@chemna.dichi.unina.it.
[†] Université Joseph Fourier.
[‡] Università Federico II.

(1) Strecker, A. *Liebigs Ann. Chem.* **1850**, *75*, 27.
(2) Mowry, D. T. *Chem. Rev.* **1948**, *42*, 189. Williams, R. M. *Synthesis of Optically Active* α*-Amino Acids*, Pergamon Press: Oxford, 1989, pp 208−229.
(3) For recent developments concerning asymmetric Strecker reactions, see: Ishtani, H.; Komiyama, S.; Kobayashi, S. *Angew. Chem., Int. Ed. Engl.* **1998**, *37*, 3186. Sigman, M. S.; Jacobsen, E. N. *J. Am. Chem. Soc.* **1998**, *120*, 4901 and 5315. Mori, M.; Imma, H.; Nakai, T. *Tetrahedron Lett.* **1997**, *38*, 6229. Iyer, M. S.; Gigstad, K. M.; Namdev, N. D.; Lipton, M. *J. Am. Chem. Soc.* **1996**, *118*, 4910.
(4) Lemmon, R. L. *Chem. Rev.* **1970**, *70*, 95. Eschenmosser, A.; Loewenthal, E. *Chem. Soc. Rev.* **1992**, 1.
(5) Miller, S. L. *Science* **1953**, *117*, 528.
(6) Miller, S. L. *Chem. Scr.* **1986**, *26B*, 5.
(7) Ponnamperuma, C.; Woeller, F. H. *Curr. Mod. Biol.* **1967**, *1*, 156. Sanchez, R. A.; Ferris, J. P.; Orgel, L. E. *Science* **1966**, *56*, 1087.

10.1021/ja9911059 CCC: $19.00
Published on Web 12/30/1999

ing from the addition of water onto formaldehyde, can be an intermediate in all these processes. Protons, which are necessary to activate OH and NH_2 as leaving groups, have been omitted in this scheme.

In this paper, we will focus our interest on the reaction of methanimine with HCN. This is the first part of a work currently in progress in our laboratories about the general picture presented in Scheme 1. We thought that this step, in which a C−C bond is formed, was of crucial importance. It might have been the first C−C bond formed in the history of life! Even though this bond could also be formed by ways (i) or (ii), kinetic studies have shown that the intermediacy of an imine in such processes is plausible.[8] Furthermore, in their attempts to develop enantioselective versions of the Strecker reaction, chemists generally use the addition of HCN (or Me_3SiCN) to preformed imines.[3] They will find some information about the mechanism of this reaction in the present paper.

Among the various scenarios proposed for the origin of life on earth, one theory emphasizes the assumption that the basic constituents of biopolymers, including the monomers of proteins, α-amino acids, may have come from space. As methanimine and hydrogen cyanide are two well-known interstellar molecules,[9] one can postulate that they might have reacted in the interstellar space, to form aminoacetonitrile, and thus to provide a source for extraterrestrial glycine. That is why the first part of this paper will be devoted to the in-vacuum reaction of HCN with methanimine in the absence of any further molecule. To the best of our knowledge, no previous quantum mechanical studies have been published about the mechanism of this reaction.

To date, amino acids have not been detected in the interstellar space, but some of them, including glycine, have been discovered on the surface of meteorites. On such surfaces, in particular on interstellar dusts, a few water molecules could modify the mechanism of the reaction between isolated HCN and methanimine. This is the subject of the second part of our study.

Coming back to the hypothesis that glycine was formed on earth, most probably in the sea, we will then present our results about the addition of HCN to methanimine in aqueous solution, using a continuum solvent model. Specific solvent effects have also been analyzed by calculations including, besides the continuum, a few explicit water molecules.

Computational Details

All the calculations were carried out using the Gaussian98 program package.[10] The equilibrium and transition structures were fully optimized by HF, B3LYP, and MP2(fc) methods using the 6-31+G(d,p) basis set.[11] B3LYP/6-31+G(d,p)-optimized geometries were used in single-point energy calculations at the B3LYP/6-311+G(3df,2p) level, while MP2/6-31+G(d,p)-optimized structures were used for QCISD(T)/6-31+G(d,p) and G2(MP2) calculations.[11] Intrinsic reaction paths (IRPs)[12] were traced starting from the various transition structures to make sure that no further intermediate exists together with those sketched in Figure 1. Harmonic frequencies of the B3LYP/6-31+G(d,p)-optimized structures were calculated in order to confirm the nature of the stationary points and to obtain zero-point energies (ZPE) and thermal corrections to enthalpies and free energies at 298.15 K in the usual rigid-rotor harmonic oscillator approximation.

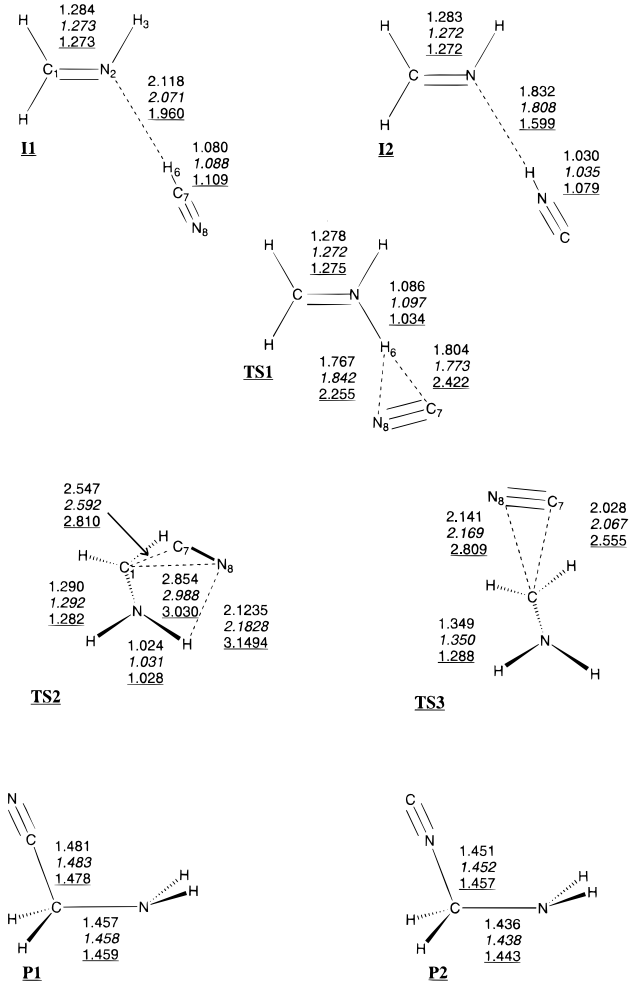

Figure 1. Optimized structures of the stationary points governing the reaction between hydrogen cyanide and methanimine according to MP2/6-31+G(d,p) (plain characters), B3LYP/6-31+G(d,p) (italic characters), and B3LYP-C-PCM/6-31+G(d,p) (underlined characters).

Three different strategies were used to investigate the role of solvent effects. At first, the solvent was considered as a macroscopic and continuous medium using the version of the polarizable continuum model (PCM) implemented by two of us in the Gaussian series of programs.[13] In this model, the variation of the free energy when going from vacuum to solution is composed of the work required to build a cavity in the solvent (cavitation energy, G_{cav}) together with the electrostatic (G_{el}) and nonelectrostatic work ($G_{disp} + G_{rep}$), connected with charging the solvent and switching on solute−solvent interactions.[13] Besides these terms (whose sum is referred to as W_0), we have taken into account the contributions to free energies issuing from the structural differences between molecules in the gas phase and in solution (W_{geom}) and from the corresponding modifications of solutes partition functions. Concerning this last term, we have assumed that translation and rotation contributions remain unmodified (i.e., that the solute has a very large volume available in solvent and that it can freely rotate),

(8) Taillades, J.; Commeyras, A. *Tetrahedron* **1974**, *30*, 2493.

(9) Delsemme, A. H. *Adv. Space Res.* **1989**, *9*, 25.

(10) Frisch, M. J.; Trucks, G. W.; Schlegel, H. B.; Scuseria, G. E.; Robb, M. A.; Cheeseman, J. R.; Zakrzewski, V. G.; Montgomery, J. A.; Stratmann, R. E.; Burant, J. C.; Dapprich, S.; Millam, J. M.; Daniels, A. D.; Kudin, K. N.; Strain, M. C.; Farkas, O.; Tomasi, J.; Barone, V.; Cossi, M.; Cammi, R.; Mennucci, B.; Pomelli, C.; Adamo, C.; Clifford, S.; Ochterski, J.; Petersson, G. A.; Ayala, P. Y.; Cui, Q.; Morokuma, K.; Malick, D. K.; Rabuck, A. D.; Raghavachari, K.; Foresman, J. B.; Cioslowski, J.; Ortiz, J. V.; Stefanov, B. B.; Liu, G.; Liashenko, A.; Piskorz, P.; Komaromi, I.; Gomperts, R.; Martin, R. L.; Fox, D. J.; Keith, T.; Al-Laham, M. A.; Peng, C. Y.; Nanayakkara, A.; Gonzalez, C.; Challacombe, M.; Gill, P. M. W.; Johnson, B.; Chen, W.; Wong, M. W.; Andres, J. L.; Head-Gordon, M.; Replogle, E. S.; Pople, J. A.; *Gaussian 98*, Revision A.6; Gaussian, Inc.: Pittsburgh, PA, 1998.

(11) Description of basis set and explanation of standard levels of theory can be found in the following: Foresman, J. B.; Frisch, Æ. *Exploring Chemistry with Electronic Structure Methods*, 2nd ed.: Gaussian, Inc.: Pittsburgh, PA, 1996.

(12) Gonzalez, C.; Schlegel, H. B. *J. Phys. Chem*. **1990**, *94*, 5523.

(13) Cossi, M.; Barone, V.; Cammi, R.; Tomasi, J. *Chem. Phys. Lett*. **1996**, *255*, 327.

whereas we have explicitly computed the variation of harmonic frequencies. As a consequence, this term will be referred to as W_{vib}.

Geometry optimizations and evaluation of harmonic frequencies have been performed using a modified version of the Gaussian package, in which improved algorithms have been introduced for the computation of first energy derivatives with respect to geometric parameters of solvated molecules[14] and analytical second derivatives can also be obtained;[15] furthermore, this version allows for a proper use of molecular symmetry even in the presence of the solvent.[16] Geometry optimizations and evaluations of Hessian matrixes were performed with the conductor variant (C-PCM),[17] whereas final energy evaluations were performed with the standard dielectric version (D-PCM) and a very refined compensation of polarization charges.[18] Since our most sophisticated procedure for generating solute cavities (united atom topological model, UATM)[18] is not fully self-consistent for reaction intermediates and transition states, we have resorted to the more conventional set of Pauling radii,[13] which, despite giving less reliable absolute values of solvation energies, is completely adequate in the evaluation of relative values for closely related species.

Then, specific solvent molecules were explicitly included in the computations both in a vacuum and including bulk solvent effects by the PCM.

To gain additional insight into the bonding characteristics of intermediates and transition structures, we have also used the atoms in molecules (AIM) theory of Bader,[19] which is based on a topological analysis of the electron density function ρ(r) and of its Laplacian $\nabla^2\rho(r)$ at the bond critical points (bcp's). Local depletion of the electronic charge ($\nabla^2\rho(r) > 0$) corresponds to interactions between closed-shell systems (ionic bond, hydrogen bond, van der Waals molecules), while the inverse ($\nabla^2\rho(r) < 0$) corresponds to covalent bonds. We have also performed a natural population analysis (NPA),[20] which yields reliable atomic charges and provides a chemical description of the bonding in terms of interactions between localized hybrid orbitals.

Results and Discussion

A. $H_2C{=}NH + HCN$ Reaction Mechanism in Vacuo. Figure 1 shows the most significant geometrical parameters of all the stationary points located both at the B3LYP/6-31+G(d,p) and at the MP2/6-31+G(d,p) levels on the potential energy surface (PES) governing addition of hydrogen cyanide to methanimine. The corresponding relative energies are collected in Table 1, and some additional information about electronic characteristics is given in Table 2.

In general terms, relative energies are little sensitive to the level of calculation, and enlargement of the basis set from 6-31+G(d,p) to 6-311+G(3df,2p) never changes B3LYP relative energies by more than 2.0 kcal mol^{-1}. From a geometrical point of view, B3LYP and MP2 models give similar trends, and from an energetic point of view, B3LYP results are close to those issuing from the very reliable (but much more expensive) G2(MP2) procedure. Thus, both AIM and NPA computations have been performed using B3LYP/6-31+G(d,p) electron densities, and adducts involving explicit water molecules have been studied at the B3LYP level only.

The first stationary point located on the PES is the **I1** complex. It presents a weak N- - -HCN hydrogen bond with a N- - -H distance of 2.118 Å at the MP2 level and of 2.071 Å at the B3LYP level. The existence of this weak bond is confirmed by both the positive value of $\nabla^2\rho(r)$ issuing from the AIM analysis (see Table 2) and the weak imine → hydrogen cyanide charge transfer (0.035 electron unit) obtained from the NPA. From an energetic point of view, **I1** is 5−7 kcal mol^{-1} more stable than the reactants. **I1** evolves to the **I2** intermediate through the C_s transition state **TS1** with a quite high energy barrier (27 kcal mol^{-1}). Full characterization of **TS1** by frequency and IRP calculations shows that it connects directly **I1** to **I2**, leading to the association of methanimine with hydrogen isocyanide. **TS1** exhibits a structure with the imine moiety almost protonated (+0.802 eu) and a N_2-H_6 covalent bond. In this connection, it is worth mentioning that the calculated proton affinity of methanimine (206.8 and 205.7 kcal mol^{-1} at the B3LYP/6-31+G(d,p) and G2 levels, respectively) is close to the computed proton affinity of NH_3 (204.0 and 204.1 kcal mol^{-1} at the G2 and CCSD(T)/6-31+G(d,p) levels, respectively), which is, in turn, in excellent agreement with the experimental value of 204 ± 1 kcal mol^{-1}.[21] Surprisingly, despite the H_6-C_7 distance around 1.8 Å, no bcp was found between H_6 and C_7; on the other hand, the AIM analysis reveals the presence of a weak N_8-H_6 bond (see Table 2). The high value of the dipole moment (10.1 D) points to the zwitterionic character of **TS1** and suggests that solvent effects could play a crucial role when the reaction occurs in a polar protic solvent, such as the aqueous ammonia solution. In **I2**, the N_2- - -H_6 bond is shorter than that in **I1** by about 0.25 Å; the value of $\rho(r)$ indicates also a stronger N_2-H_6 hydrogen bond (0.0399 vs

Table 1. Relative Energies (kcal mol^{-1}) of the Stationary Points Governing the Reaction between Methanimine and Hydrogen Cyanide in a Vacuum

structure	HF[a,b]	B3LYP[a,b,c]	MP2[a,b]	QCISD(T)[a,b]	G2MP2[a]
I1	−6.5	−6.8 (−6.0)	−7.2	−7.0	−5.1
TS1	25.8	25.7 (26.2)	27.1	27.2	27.1
I2	0.7	2.9 (4.3)	6.8	4.5	5.8
TS2	28.4	32.2 (32.3)	35.5	35.2	36.1
P1	−25.5	−26.5 (−27.1)	−27.1	−23.1	−21.6
TS3	-	22.0 (23.5)	27.0	27.1	28.2
P2	−11.7	−9.2 (−7.1)	−6.3	−6.5	−3.7

[a] With respect to reactants, whose total energies (Hartree) are −186.92086 (HF), −188.07122 (−188.12929) (B3LYP), −187.52099 (MP2), −187.57342 (QCISD(T)), −187.63608 (G2(MP2). [b] Using the 6-31+G(d,p) basis set. [c] Values in parentheses correspond to single-point calculation using the 6-311+G(3df,2p) basis set.

Table 2. Calculated Charge Transfer q (Electron Unit),[a] Dipole Moment μ (Debye), and Bond Critical Point (bcp) Analysis in the Stationary Points Governing the Reaction between Methanimine and Hydrogen Cyanide in a Vacuum (All Calculations Performed at the B3LYP/6-31+G(d,p) Level)

structures	q	μ	bond	$\rho(r)_{bcp}$	$\nabla^2\rho(r)^b$
I1	−0.035	6.3	N_2-H_6	0.023	0.058
TS1	−0.802	10.1	N_2-H_6	0.265	−1.312
			N_8-H_6	0.050	0.086
			N_8-H_4	0.014	0.049
I2	−0.124	6.9	N_2-H_6	0.040	0.092
TS2	−0.803	9.0	N_2-H_8	0.020	0.064
P1	−	2.6	C_1-C_7	0.256	*−0.655*
TS3	−0.527	5.9	C_1-N_8	0.067	0.073
P2	−	2.6	C_1-N_7	0.249	*−0.594*

[a] Amount of charge transfer from $H_2C{=}NH$ (or $H_2C{=}NH_2^+$) to HCN (or CN^-); a negative value indicates electron transfer from $H_2C{=}NH$ to HCN. [b] See Figure 1 for atom numbering.

(14) (a) Barone, V.; Cossi, M.; Tomasi, J. *J. Comput. Chem.* **1998**, *19*, 404. (b) Mennucci, B.; Cances, E.; Tomasi, J. *J. Phys. Chem. A* **1997**, *101*, 10506.

(15) Cossi, M.; Barone, V. *J. Chem. Phys.* **1998**, *109*, 6246.

(16) Scalmani, G.; Barone, V. *Chem. Phys. Lett.* **1999**, *301*, 263.

(17) Cossi, M.; Barone, V. *J. Phys. Chem. A* **1998**, *102*, 1995.

(18) Barone, V.; Cossi, M.; Tomasi, J. *J. Chem. Phys.* **1997**, *107*, 3210.

(19) Bader, R. F. W. *Atoms in Molecules. A Quantum Theory*; Oxford University Press: Oxford, U. K., 1990.

(20) Curtiss, L. A.; Pochatko, D. J.; Reed, A. E.; Weinhold, F. *J. Chem. Phys.* **1983**, *82*, 2679. See also: Reed, A. E.; Curtiss, L. A.; Weinhold, F. *Chem. Rev.* **1988**, *88*, 899.

(21) (a) Curtiss, L. A.; Raghavachari, K.; Trucks, G. W.; Pople, J. A. *J. Chem. Phys.* **1991**, *94*, 7221. (b) Peterson, K. A.; Xantheas, S. S.; Dixon, D. A.; Dunning, T. H., Jr. *J. Phys. Chem. A* **1998**, *102*, 2449.

Table 3. Relative Thermodynamic Contributions (kcal mol^{-1}) at 298.15 K for the Stationary Points Governing the Reaction between Methanimine and Hydrogen Cyanide in a Vacuum[a]

			ΔH		ΔG	
structure	Δ(ZPE)	$-T\Delta S$	B3LYP	G2(MP2)	B3LYP	G2(MP2)
I1	1.3	7.2	−5.6	−3.9	1.6	3.3
TS1	1.3	9.3	26.1	27.5	35.4	36.8
I2	1.4	7.8	4.1	5.7	11.9	13.5
TS2	2.4	9.4	33.8	37.7	43.2	47.1
P1	4.6	10.4	−23.1	−18.2	−12.7	−7.8
TS3	2.9	10.0	23.9	30.1	33.9	40.1
P2	4.5	10.3	−5.8	−0.3	4.5	10.0

[a] With respect to reactants, whose ZPE, $T\Delta S$, ΔH, and ΔG values are 35.3, 30.6, 39.9, and 9.3 kcal mol^{-1}.

0.0234).[22,23] This increase of the association's strength is confirmed by the larger charge transferred from imine to HNC in **I2** (0.035 and 0.124 for **I1** and **I2**, respectively). From **I2**, the cyano addition proceeds through **TS2** with an energy barrier of about 30 kcal mol^{-1}. The AIM analysis, as well as the geometrical structure of TS2, suggests that the H_6-N_8 bond in the HNC moiety has not been fully broken ($\rho(r) = 0.0203$), whereas the same method does not evidence any bond between the carbon or the nitrogen of the cyano group and the attacked carbon atom C_1. The cyano addition to the ammonium ion is achieved for the **P1** product, the most stable structure of the whole PES. The isocyano product **P2** is, indeed, less stable than **P1** by about 18 kcal mol^{-1} according to both B3LYP and G2-(MP2) methods. Along the pathway leading to **P1**, the reaction energy varies between −21.6 and −27.0 kcal mol^{-1}, depending on the level of calculation. However, one can notice that, according to the IRP traced at the HF level, **TS2** leads to the isocyano product **P2**, whereas at the B3LYP and MP2 levels, **P2** is obtained via **TS3**. This latter transition structure is slightly tighter, with an average interfragment distance of 2.1 Å. Electron density $\rho(r)$ and its Laplacian$\nabla^2\rho(r)$ seem to explain the evolution of **TS3** toward **P2** better than geometric parameters. For instance, even though the shortest distance is found between the C_1 and C_7 atoms, the AIM analysis reveals only a weak bond between C_1 and N_8 atoms (see Table 2). The zwitterionic character of **TS3** is less pronounced than those of **TS1** or **TS2**, the dipole moment of **TS3** being as low as 5.9 D.

We next used standard procedures to evaluate nonpotential energy terms at 298.15 K and 1 atm; the results are summarized Table 3.

Relative enthalpies at 298.15 K are larger than relative electronic energies for all the reaction channels, the difference ranging between 1.2 and 3.4 kcal mol^{-1}. On the other hand, entropy contributions do favor the reaction. Proper inclusion of all these terms leads to the free energy profile shown in Figure 2, in which **I1** and **P2** are less stable than reactants and large activation energies govern both the first and the second elementary step. The free energy of the highest transition state (TS2) is 43.2 (B3LYP) or 47.1 (G2MP2) kcal mol^{-1} above that of the reactants, so that addition of HCN to methanimine in the gas phase is a quite difficult process and, in particular, the computed energy barriers are too high to allow the formation of HNC in the interstellar space.

B. $H_2C{=}NH + HCN$ Reaction Mechanism in Aqueous Solution. 1. Continuum Approach. In this section, the influence of bulk solvent and its consequences on the geometric and energetic features of the reaction will be analyzed. The main

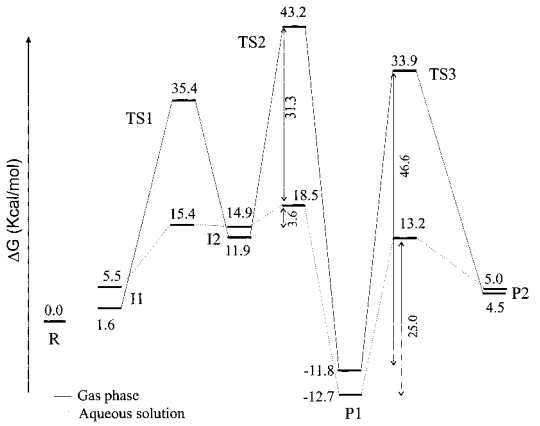

Figure 2. Free energy profiles for the reaction between hydrogen cyanide and methanimine in the gas phase and in aqueous solution.

geometric parameters of all the stationary points located using the PCM representation of aqueous solution are compared in Figure 1 to their counterparts computed in a vacuum. The relative Gibb's energies in aqueous solution are collected in Table 4, and the free energy profile is sketched in Figure 2.

The results shown in Figure 1 are indicative of the large changes induced by the solvent on the interfragment distances. For instance, the intermolecular N_2- - -H_6 bond is shortened in solution by 0.1 and 0.2 Å for **I1** and **I2,** respectively, and at the same time, the C−H bond of HCN and the N−H bond of HNC are lengthened. Thus, in aqueous solution, **I1** and **I2** are best prepared for proton transfer between both fragments. These trends are even more striking for the transition structures, which are characterized by interfragment distances larger by 0.4−0.7 Å in solution than those in the gas phase. These effects are clearly related to the preferential stabilization of structures involving charge separation by polar solvents. On the other hand, as expected, the geometrical structures of **P1** and **P2** are only slightly affected by the solvent.

Despite the large differences between some geometrical parameters optimized in the gas phase and in solution, inspection of Table 4 shows that the majority of solvent stabilizing effects are obtained using gas-phase structures. The comparison of the free energy profiles in a vacuum and in aqueous solution (Figure 2) clearly shows that the transition states are strongly stabilized through the electrostatic effect of the solvent. On the other hand, intermediates and products are slightly destabilized. As a result, **I1** is predicted to be unstable under normal temperature and pressure conditions. The imaginary frequencies at the transition states (ω^+) give some indication of the "rigidity" of these structures and can be used also to obtain a rough estimate of tunneling effects through the Wigner expression of the transmission coefficient $\chi(T)$, which multiplies the conventional rate constant.[24] The imaginary frequencies of Table 4 confirm that TSs become significantly looser in aqueous solution and that tunneling effects can be safely neglected in the present context. More generally, zero-point energies and thermal effects are comparable in a vacuum and in solution and never play a dominant role in determining general trends.

In summary, the reaction seems much easier in aqueous solution than in the gas phase: the second step is rate-determining in both cases, but the activation free energy is reduced by about 25 kcal mol^{-1} by the presence of water.

2. Supermolecule Approach Including Explicit Water Molecules. It is well documented that contemporary continuum

(22) Koch, U.; Popelier, P. L. A. *J. Phys. Chem.* **1995**, *99*, 9747.

(23) Mo, O.; Yanez, M.; Elguero, J. *J. Chem. Phys.* **1992**, *97*, 6628. Alkorta, I.; Elguero, J. *J. Phys. Chem.* **1996**, *100*, 19367.

(24) Eyring, H.; Lin, S. H.; Lin, S. M. *Basic Chemical Kinetics*; Wiley: New York, 1980.

Table 4. Different Free Energy Contributions at 298 K (kcal mol^{-1}) and Transition Frequencies of TSs (cm^{-1}) for the Stationary Points Governing the Reaction between Methanimine and Hydrogen Cyanide in Aqueous Solution (See Text for Details)[a,b]

	ΔG_{vac}							ΔG_{sol}	
structure	B3LYP	G2(MP2)	ΔW_0	ΔW_{geom}	ω^+_{vac}	ω^+_{sol}	ΔW_{vib}	B3LYP	G2(MP2)
I1	1.6	3.3	3.9	0.0			0.0	5.5	7.2
TS1	35.4	36.8	−16.5	−3.7	203i	70i	0.2	15.4	16.8
I2	11.9	13.5	3.3	0.7			0.4	14.9	16.5
TS2	43.2	47.1	−18.5	−4.4	378i	202i	−1.8	18.5	22.4
P1	−12.7	−7.8	0.9	0.4			−0.4	−11.8	−6.9
TS3	33.9	40.1	−3.6	−15.3	322i	117i	−1.8	13.2	19.4
P2	4.5	10.0	2.7	1.2			−3.4	5.0	10.5

[a] With respect to reactants for which $W_0 = -9.3$ kcal mol^{-1}, $W_{geom} = -9.5$ kcal mol^{-1}, and $W_{vib} = 0.1$ kcal mol^{-1}. [b] $\Delta G_{sol} = \Delta G_{vac} + \Delta W_0 + \Delta W_{geom} + \Delta W_{vib}$.

models are adequate to describe reactions in solution unless some solvent molecules are directly involved in the reaction mechanism (e.g., through a concerted proton transfer). Preliminary calculations indicate that no water molecule acts as a proton relay, but that one or two water molecules can be involved in relatively strong hydrogen bonds linking the reactants. This prompted us to locate all the stationary points on the potential energy surface governing the reaction between hydrogen cyanide and ethanimine in the presence of two explicit water molecules.

The B3LYP/6-31+G(d,p)-optimized structures of the stationary points are collected in Figure 3; their relative electronic and nonpotential energies are summarized in Table 5. Some additional information on the electronic structure and bonding properties of the critical points is reported in Table 6. Since extension of the basis set up to the 6-311+G(3df,2p) level has a negligible effect (see Table 5), we will explicitly refer in the following only to 6-31+G(d,p) results.

In the first intermediate, **Ia**, the reactants are linked together by the two water molecules. Geometrical parameters, as well as the AIM analysis, indicate the presence of strong hydrogen bonds involving the O_7 and H_8 atoms of W1, whereas no direct bond is found between H_6 and N_2 atoms belonging to HCN and the imine moiety, respectively. From an energetic point of view, **Ia** is 9.5 kcal mol^{-1} more stable than the reactant molecules solvated separately by one water molecule. The analogue of **I1**, named here **Ib** (association complex between the methanimine and the hydrogen cyanide), is obtained through the displacement of the water molecule W2 toward H_3 via **Tsab**. The hydrogen-bonding between H_6 and N_2 is already present in **Tsab** ($\rho(r) = 0.0222$) and almost achieved in **Ib** ($\rho(r) = 0.0285$). For this step, the computed energy barrier is 8.0 kcal mol^{-1}. The formation of a zwitterionic form ($H_2C{=}NH_2^{\delta+}$,$CN^{\delta'-}$) is obtained during the successive step, which leads to **Ic** via **TSbc**, with a loss of 0.849 electrons on the $H_2C{=}NH_2$ fragment and an excess of 0.787 electrons on the CN fragment. Bond lengths and $\rho(r)$ values give concordant results, and both predict a strengthening of the intermolecular interactions between the solute and water molecules. The energy barrier for this step is reduced by 8.0 kcal mol^{-1} with respect to that of the gas phase (**TS1**). Then **Ic** can evolve according to two different pathways.

In the first one the water molecule W1 is shifted toward the NH_2 end of the iminium ion to give an H_6- - -O_7 hydrogen bond; at the same time, the cyano group turns off the iminium plane (**TScd**). The "out-of-plane" equilibrium geometry is achieved in the intermediate **Id** strongly stabilized by hydrogen bonds (for example, compare in Table 6 the $\rho(r)$ values at the O- - -H bcp in **Ic** and **Id**: $\rho(r)$ (H_5- - -O_7) = 0.0139 (**Ic**); $\rho(r)$ (H_6- - -O_7) = 0.0481 (**Id**)). This part of the potential energy surface is rather flat, with an energy difference between energy minima of 1.0 kcal mol^{-1} and an energy barrier of 2.4 kcal mol^{-1} for the migration out of the iminium plane toward the CH_2 end.

Table 5. Relative B3LYP Electronic Energy (ΔE), Zero-Point Vibrational Energy (ΔZPE), Enthalpy (ΔH), Entropy Contribution ($-T\Delta S$), Gibb's Free Energy in Vacuum (ΔG), Solvent Contribution to Free Energy (ΔW_0), and Free Energy in Solution (ΔG_{sol}) for the Stationary Points Governing the Reaction between Methanimine and Hydrogen Cyanide in the Presence of Two Water Molecules[a] (All Values in kcal mol^{-1})

structure	ΔE[b]	ΔZPE	ΔH	$-T\Delta S$	ΔG	ΔW_0	ΔG_{sol}[c]
Ia	0.0	0.0	0.0	0.0	0.0	0.0	0.0
TSab	8.0 (6.1)	−1.2	7.1	−0.7	6.4	−2.6	3.8
Ib	5.9 (4.3)	−1.2	5.6	−3.1	2.5	−2.2	0.3
TSbc	17.7 (17.9)	0.9	17.5	3.5	21.0	−10.9	10.1
Ic	14.9 (15.0)	1.3	15.4	2.9	18.3	−9.0	9.3
TScd	15.9 (15.7)	1.5	15.7	5.0	20.7	−10.3	10.4
Id	13.6 (14.0)	1.4	13.5	4.4	17.9	−10.4	7.5
TSde	16.0 (16.3)	1.8	16.2	5.3	21.5	−7.5	14.0
Ie	15.1 (15.3)	2.3	16.4	3.8	20.2	−7.3	13.9
TSef	15.9 (16.1)	2.2	16.8	4.6	21.4	−5.2	16.2
Pf	−15.1(−14.8)	2.4	−13.0	1.6	−11.4	−2.2	−13.6
TScg	16.2 (16.4)	−0.1	15.3	2.8	18.1	−10.3	7.8
Ig	14.7 (14.6)	−1.3	13.9	−1.2	12.7	−1.6	11.1

[a] For **Ia**, $E = -340.97495$ (−341.08209) au; ZPE = 0.107125 au; $-TS = 0.054\ 55$ au; $W_0 = -8.7$ kcal mol^{-1}. [b] Values in parentheses correspond to single-point calculation using the 6-311+G(3df,2p) basis set. [c] $\Delta G_{sol} = \Delta W_0 + \Delta G$.

For this latter transition structure **TSde**, no bonding between the methaniminium and the cyano group was detected, while for the intermediate **Ie** connected to **TSde** the AIM analysis suggests a weak bonding between the C_1 atom and the N_{11} atom (see Figure 3 and Table 6). The last step of this pathway leads to the formation of the C−C bond. The corresponding transition structure **TSef** lies only 0.8 kcal mol^{-1} above **Ie** and is reached for a large C_1- - -C_{10} distance (2.422 Å). AIM analysis also indicates a weak bonding between these two carbon atoms ($\rho(r) = 0.0303$, $\nabla^2\rho(r) > 0$). At the same time, hydrogen bonds involving W1 and W2 are weakened. The small charge transfer from CN to H_2CNH_2 (0.031 eu) confirms the early character of this TS, in agreement with the exothermicity of this step (−30.2 kcal mol^{-1}). As expected, the strength of the hydrogen bonds between the water molecules W1 and W2 and the addition product (**Pf**) is strongly reduced ($\rho(r) < 0.01$). The overall reaction is 8 kcal mol^{-1} less exothermic than the corresponding process in the gas phase.

The second pathway issuing from **Ic** leads to the intermediate **Ig** (i.e., the association between methanimine and hydrogen isocyanide corresponding to **I2** in a vacuum). However, despite the intermolecular N_2- - -N_6 distance being shorter in **Ig** and a rather large value of $\rho(r)$ (0.0679 vs 0.0285), the energy differences between **Ig** and **Ib** on one hand, and **I2** and **I1** on the other hand, are comparable (8.8 vs 9.7 kcal mol^{-1}). **TScg**, which connects **Ic** and **Ig**, corresponds to a small motion of the CN group in the iminium plane, with a N_{11}- - -H_6 bond displaying already a covalent character ($\rho(r) = 0.1089$, $\nabla^2\rho(r)$

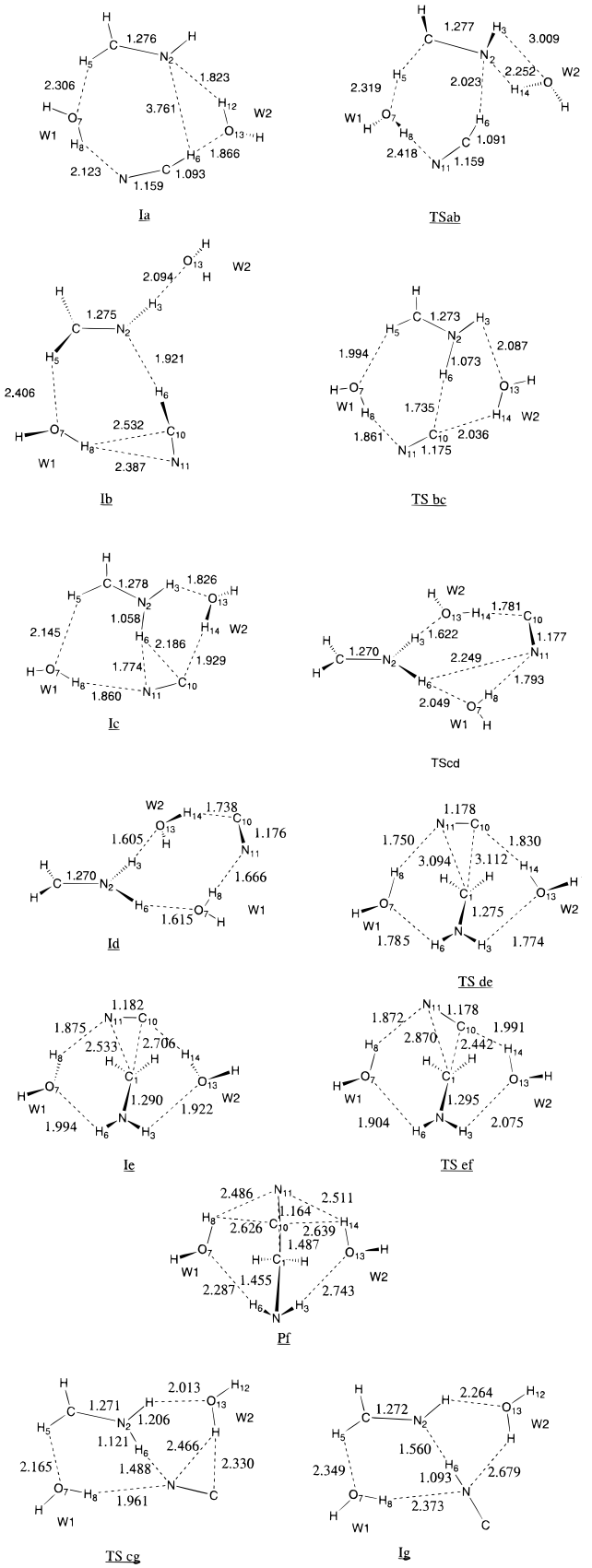

Figure 3. Optimized structures of the stationary points governing the reaction between hydrogen cyanide and methanimine in the presence of two water molecules.

Table 6. Population and Bond Critical Point (bcp) Analyses for the Stationary Points Governing the Reaction between Methanimine and Hydrogen Cyanide in the Presence of Two Water Molecules (All Calculations Performed at the B3LYP/6-31G+(d,p) Level)

structure	q_{W1}	q_{W2}	$q_{(H)CN}$	bond	$\rho(r)_{bcp}$	$\nabla^2\rho(r)^a$
Ia	−0.005	−0.016	−0.028	H_5-O_7	0.009	0.054
				H_8-N_{11}	0.014	0.066
				H_6-O_{13}	0.026	0.147
				N_2-H_{12}	0.033	0.151
TSab	0.001	−0.006	−0.035	H_5-O_7	0.009	0.052
				H_8-N_{11}	0.009	0.041
				N_2-H_6	0.022	0.108
				N_2-H_{10}	0.012	0.056
Ib	−0.003	0.014	−0.050	H_5-O_7	0.007	0.029
				H_8-N_{11}	0.009	0.043
				N_2-H_6	0.029	0.136
				H_3-O_{13}	0.015	0.080
TSbc	−0.018	−0.041	−0.755	H_5-O_7	0.024	0.071
				H_8-N_{11}	0.032	0.084
				H_6-C_{10}	0.051	0.059
				H_3-O_{13}	0.020	0.073
				$C_{10}-H_{14}$	0.029	0.059
Ic	−0.025	−0.037	−0.787	H_5-O_7	0.014	0.080
				H_8-N_{11}	0.031	0.123
				H_6-N_{11}	0.039	0.102
				H_3-O_{13}	0.028	0.140
				$C_{10}-H_{14}$	0.029	0.082
TScd	−0.028	−0.048	−0.785	H_6-O_7	0.016	0.081
				H_6-N_{11}	0.013	0.053
				H_3-O_{13}	0.048	0.194
				$C_{10}-H_{14}$	0.045	0.092
				H_8-N_{11}	0.036	0.140
Id	−0.001	−0.058	−0.757	H_6-O_7	0.048	0.200
				H_3-O_{13}	0.050	0.197
				$C_{10}-H_{14}$	0.050	0.095
				H_8-N_{11}	0.048	0.165
TSde	−0.015	−0.058	−0.795	H_6-O_7	0.031	0.152
				H_3-O_{13}	0.032	0.153
				$C_{10}-H_{14}$	0.039	0.091
				H_8-N_{11}	0.039	0.144
Ie	−0.016	−0.046	−0.749	H_6-O_7	0.019	0.102
				C_1-N_{11}	0.021	0.081
				H_3-O_{13}	0.022	0.115
				$C_{10}-H_{14}$	0.030	0.084
				H_8-N_{11}	0.028	0.114
TSef	−0.010	−0.039	−0.718	H_6-O_7	0.023	0.122
				C_1-C_{10}	0.030	0.074
				H_3-O_{13}	0.016	0.089
				$C_{10}-H_{14}$	0.025	0.076
				H_8-N_{11}	0.027	0.112
Pf	0.003	0.003	-	H_6-O_7	0.009	0.053
				H_3-O_{13}	0.009	0.055
				$N_{11}-H_{14}$	0.008	0.037
				H_8-N_{11}	0.008	0.039
TScg	−0.029	0.001	−0.678	H_5-O_7	0.014	0.076
				H_3-O_{13}	0.018	0.104
				$C_{10}-H_{14}$	0.011	0.046
				H_8-N_{11}	0.026	0.085
				H_6-N_{11}	0.109	0.065
Ig	0.001	0.005	−0.131	H_6-O_7	0.008	0.050
				N_2-H_6	0.068	0.244
				H_3-O_{13}	0.010	0.062
				$N_{11}-H_{14}$	0.005	0.023
				H_8-N_{11}	0.009	0.042

[a] See Figure 3 for atom numbering.

< 0). **TScg** lies 1.3 kcal mol^{-1} above **Ic** and 1.5 kcal mol^{-1} above **Ig**. Thus, at this level of calculation, this step can be considered reversible.

As shown in Table 5, the inclusion of nonpotential energy terms modifies the energetic diagram obtained using the electronic energies. For some stationary points (**TSab**, **TScg**, **Ig**), ΔH is about 1 kcal mol^{-1} lower than ΔE, while for some others (**Ie**, **TSef**, **Ig**), ΔH is 1 kcal mol^{-1} or more larger than ΔE. Entropy contributions favor only the first step of the proposed mechanism. These contributions give the Gibbs energy profile shown in Figure 4.

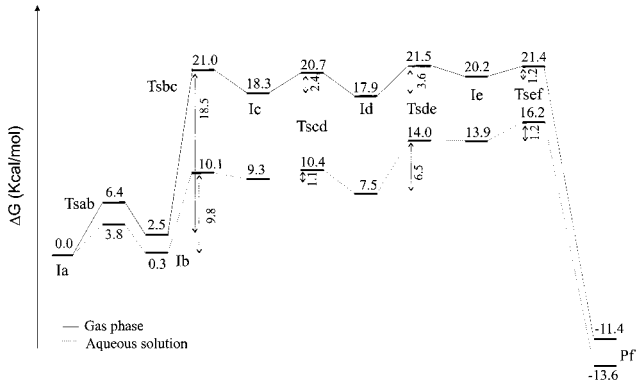

Figure 4. Free energy profiles for the reaction between hydrogen cyanide and methanimine in the presence of two water molecules without and with bulk solvent effects.

At this level, the structure **Ic** is predicted to be unstable, and **TScg** is not a transition structure. The first step still corresponds to the dissociation of HCN (**TSbc** vs **TS1**), but the following steps of the water-assisted and vacuum reactions differ notably from both energetic and mechanistic points of view. The $\Delta G^{\ddagger}$ of the whole reaction is strongly reduced (21.4 vs 43.2 kcal mol^{-1}) in the presence of two water molecules but remains 2.9 kcal mol^{-1} higher than the value obtained using the continuum approach. This free energy barrier does not agree with the hypothesis that HCN and methanimine, in the presence of water molecules, react to give the aminoacetonitrile in a gas-phase process.

We examine now the effect of the bulk solvent reaction field on the energetics of the water-assisted addition of hydrogen cyanide to methanimine. As our previous results have shown that even important geometrical changes have little influence on the solvation energy, and considering the difficulties in locating TSs (related to the extreme softness of some degrees of freedom of the water molecules), bulk solvent effects have been estimated using the gas-phase optimized geometries depicted in Figure 3. The results are summarized in Table 5. Free energies of solvation ΔG(s) remain important and provide a stabilizing effect. The least stabilized structure is **Ia,** whereas all the structures involving large charge separations are significantly stabilized. Consequently, the process is more exoergic by 2.2 kcal mol^{-1}, and the free energy barrier governing the reaction is reduced to 16.2 kcal mol^{-1}. The inclusion of bulk solvent effects also induces some modifications on the free energy profile of the reaction. The most important one is the large stabilization of **TScg**, which involves a significant charge separation. Comparison of Figures 2 and 4 shows that the addition of two explicit water molecules lowers the free energy barrier of the rate-determining step by 2.3 kcal mol^{-1} (16.2 vs 18.5 kcal mol^{-1}) and increases the exoergicity of the overall process by 0.9 kcal mol^{-1}. Thus, a correct reproduction of solvent effects requires a discrete/continuum model including both specific and bulk contributions.

Conclusion

In this paper we have reported a comprehensive study of the addition reaction of hydrogen cyanide to methanimine both in the gas phase and in aqueous solution. Our results can be summarized as follows:

(1) In the gas phase, the reaction is a stepwise process where an intermediate involving an association between methanimine and hydrogen isocyanide plays a key role. Because of the large activation energy, this addition is very unlikely to occur in the interstellar space.

(2) Bulk solvent effects, described by the polarizable continuum model, induce large geometrical changes and significant stabilization of transition structures which involve much larger charge polarization than the corresponding energy minima. As a consequence, the activation free energy of the rate-determining step is reduced by about 25 kcal mol^{-1}, even if the general reaction mechanism is comparable to that found in the gas phase.

(3) Specific solvent effects were next taken into account, including in the computations two explicit water molecules. Our results indicate that water molecules are not involved in a proton relay mechanism but simply favor the approach of reacting molecules through the formation of hydrogen bridges. With respect to the gas phase, the inclusion of two water molecules leads to a significant lowering of the free energy barrier (21.5 vs 43.2 kcal mol^{-1}) and to some modification of the reaction mechanism.

(4) Specific and bulk contributions work together in determining the overall effect of the aqueous medium on the title reaction. Our most complete model including both terms leads to an activation free energy of 16.2 kcal mol^{-1}, i.e., much lower than the value computed for the isolated system.

(5) Together with their intrinsic interest, our results show that we dispose of a general and reliable computational strategy for the study of chemical reactions in aqueous solution. This is even more promising taking into account the very good agreement between density functional and refined post-HF results and the computational efficiency of our version of PCM. Since all these procedures are being implemented in the framework of linear scaling procedures and of QM/MM methods, also very large systems will be shortly amenable to this kind of studies.

JA9911059